# DIFFERENTIAL PATTERNS OF MICROGLIAL REACTIVITY IN ACCORDANCE WITH NEURODEGENERATIVE DISEASE TYPES – A COMPARATIVE STUDY

D. Havas, J. Pindjakova, T. Hanania, I. Morganstern *PsychoGenics Inc., Paramus, NJ USA*

**PsychoGenics**
*Redefining Drug Discovery Through Innovation*

## INTRODUCTION

Microglial activation is commonly seen as one major part of neuroinflammation. When activated microglia seem to undergo a series of stadia, pending on their current 'task'. Today's knowledge about microglial morphology and activation states vastly relies on in vitro cell culture experiments. Criticism to those theories rose steadily during the last decade, especially when looking at post mortem conditions in brain tissue.

The probably most commonly accepted view on microglial states was summarized by Karperien et al. 2011 (Fig. 1), whereas the authors also critically review the comparability of measurements and interpretations. To stress the thesis, we developed a tool set of methods to measure and classify microglia and compare them in ex vivo CNS samples of different disease mouse models of AD, Tauopathy, ALS and Rett Syndrome.
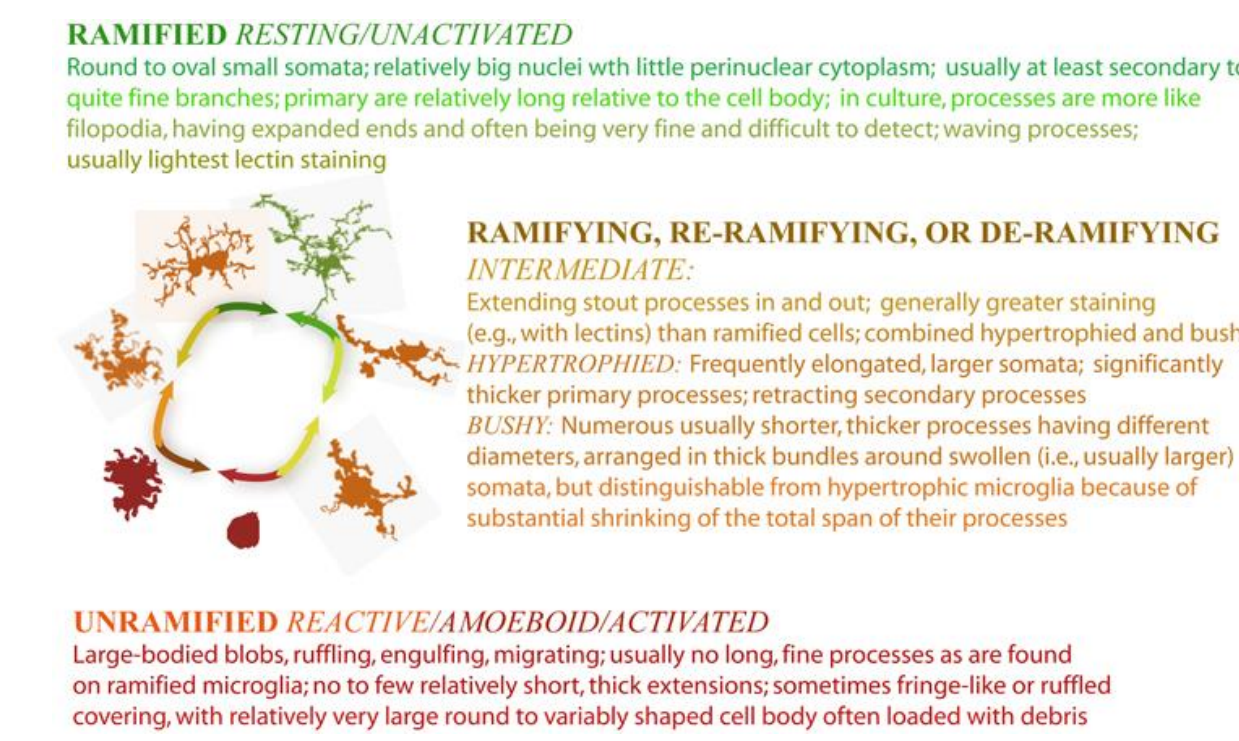
**Figure 1:** Well accepted frame work defining the stages of microglia related to most probable functionality (Karperien et al. 2011).

## METHODS

**ANIMALS:** Tested mice were transgenic vehicle controls and wild type littermates or tTA controls (for Tg4510) from several preclinical histological studies. Those include female Tg4510 mice (age 6M, n = 10), 3xTg mice (age 6M, n = 4), male SOD1G93A (Hi) mice (age 16we, n = 4) and female BIRD Mecp2+/- mice (age 14we, n = 8). Data are either shown for the cerebral cortex, frontal cortex or spinal cords (ALS).

**BRAIN SAMPLES:** Brain hemispheres were collected according to PGI' standard procedures. In short, mice were flush perfused with saline or PBS to remove blood cells before harvest. Brain hemispheres were cryoprotected in 15% sucrose after post fixation in 4% phosphate buffered PFA and frozen within OCT in molds in dry ice cooled liquid isopentane. Blocks were cut according to a uniform systematic random sampling (USR) protocol and 5 to 7 sagittal 10 micron thick USR sections were investigated per animal.

**MEASUREMENTS:** Evaluations of microglia were based on three pillars: (A) classical Iba1 counting (density, signal, overall IR surface area asf. Fig. 2) widened with (B) a four type classification (Fig. 3) by computer learned algorithms ('clustered', 'large ramifying', 'small ramifying' and 'ramified resting') and (C) additional structural soma-branch analysis ('SBA'; Fig. 4) of 'somal size', 'branching' and 'process lengths'. Together those data define a pattern of microglial reactivity, whereas the data are always shown as percent change from controls.
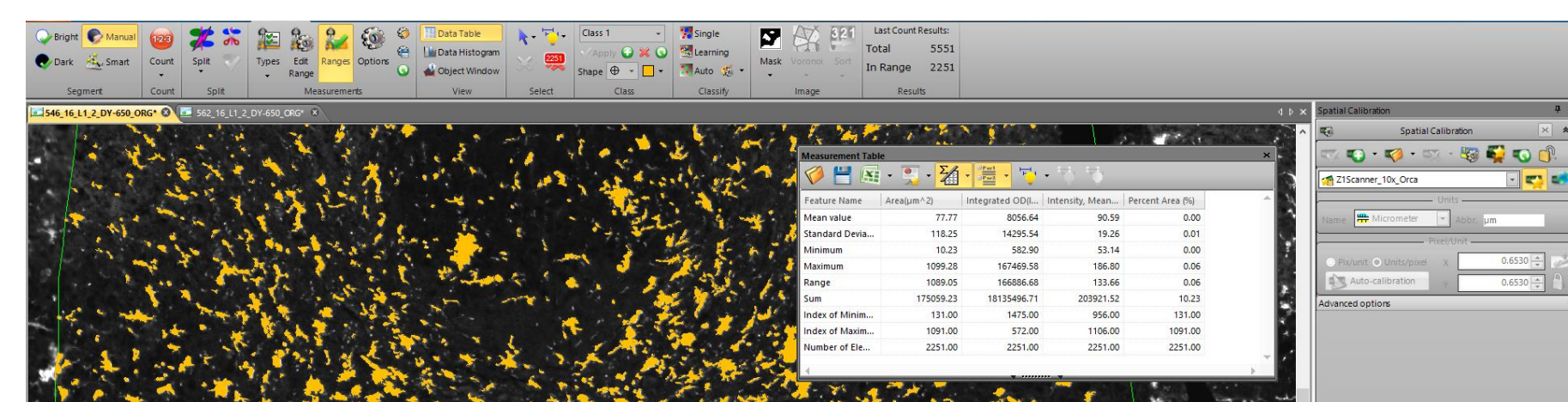
### Classical Iba1 Measurements

**Figure 2:** Classical histological Iba1 evaluations: All objects above minimal size and threshold are counted within a region of interest (ROI). A series of different variables can be extracted from this count. The best known are IR surface area in percent of the ROI size, the mean signal intensity of objects, object density, average object size, and integrated object density (mean signal x size of each object).

### Computer Learned MG Classification

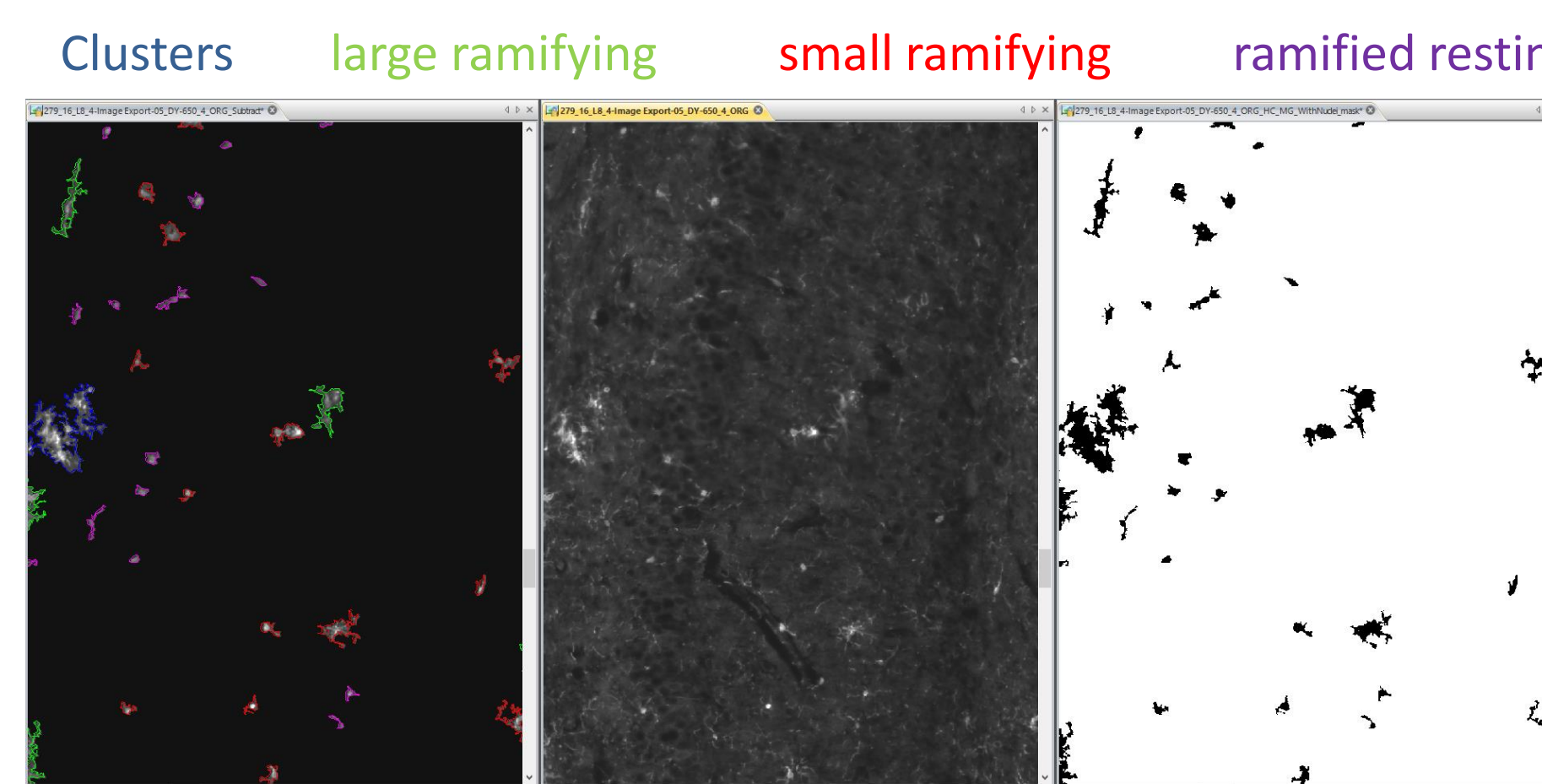Clusters · large ramifying · small ramifying · ramified resting

**Figure 3:** Right: Classification recipe of microglial cells according to computer learned weighted algorithms using parameters such as signal intensity, standard deviation of signal, IOD, mean diameter, clumpiness, size, relative size, heterogeneity, margination, circularity and aspect ratio. Left: The extracted cell mask (right) of microglial cells containing nuclei within the section) is subtracted from the original (middle) and then classified (left) according to a saved recipe.
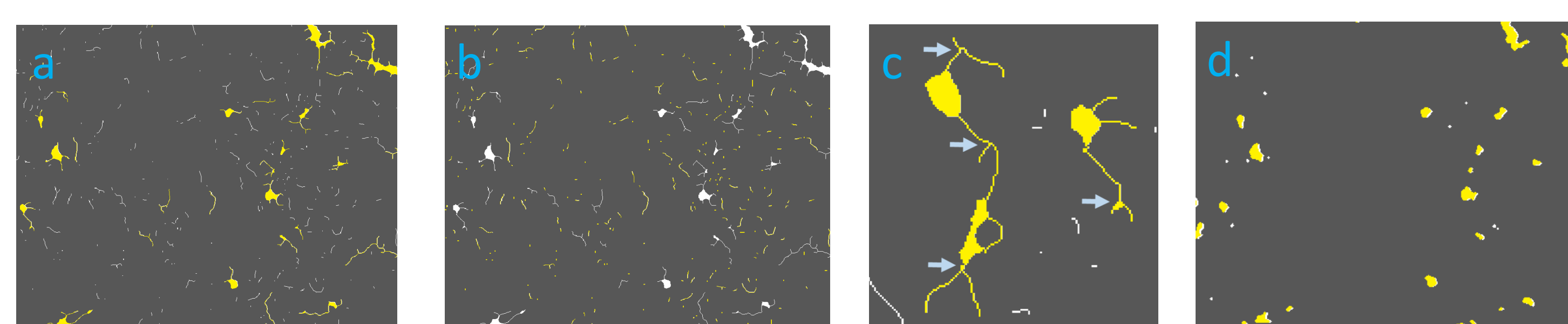
### Soma – Branch –Analysis (SBA)

**Figure 4:** Microglia SBA: Measured objects for the different steps of the SBA are shown with a yellow fill, (a) the determination of processes adjacent to somata and their branching, b) single pixel processes that are not adjacent to somata und unbranched. Arrows in (c) point at branching points to clarify the detail how the software determines branches. (d) shows the measurement of somata alone.
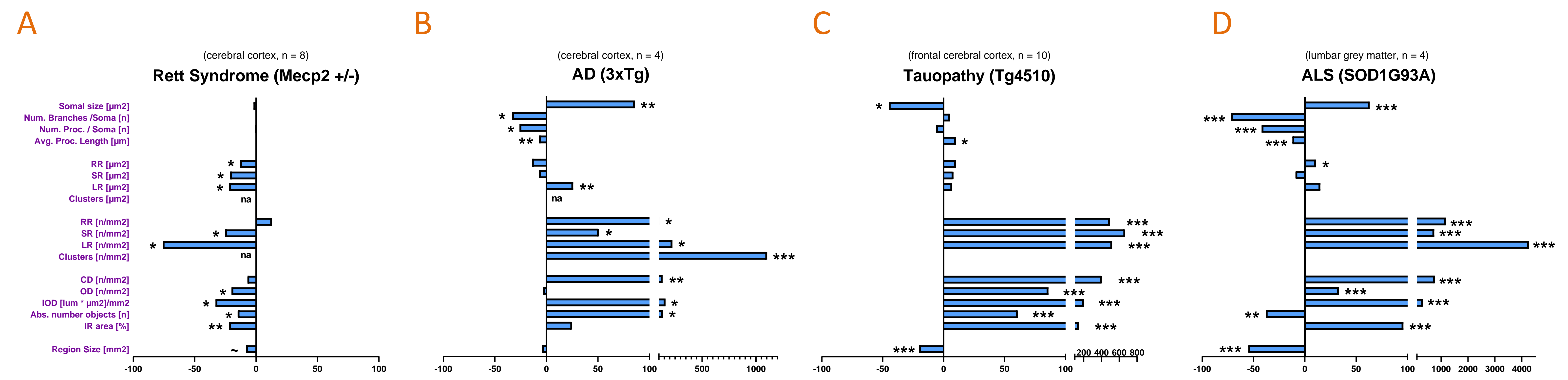
## RESULTS

**Figure 5:** Left to right: Pattern plots to visualize the percent change of the same variables in the different disease models versus wildtype (or tTA) controls. Variables are selected and thus incomplete. For each model additional variables exist being as well distinctive. However, the selected variables allow a substantial comparison of the patterns from the different disease models. (A) Rett mice are described as immune deficient. The obtained results for microglia confirm that Iba1 is generally lower and that all basic morphological forms associated with NI are reduced (e.g. density of small and large ramifying cells). More important branching and process lengths stay unaltered, which could hint at a general disability of microglia to de- or hyper-ramify. (B) 3xTg mice as AD model feature amyloidosis paired with a certain degree of Tauopathy. As only model we see AD typical clustering of microglia and a general cytosis. Notably these mice show a clear pattern of de-ramification in an early stage without cortical atrophy. (C) The mere Tauopathy leads to a clear atrophy. Also in this model a strong microglial cytosis is present without clustering. In contrast to the AD model, somal size decreases and cells are not de-ramified at this later stage. Average process length is even significantly increased. (D) The ALS model features a similar but greater de-ramification pattern compared to the AD model, but does not show much clustering and stands out for an extreme increase of large ramifying microglia (>40-fold). 'na' = determined but incomparable (none in WT). ~ = p<0.1; * = p<0.05; ** = p<0.01; *** = p<0.001. Significances from unpaired two-tailed t-test or Tukey's post hoc test.

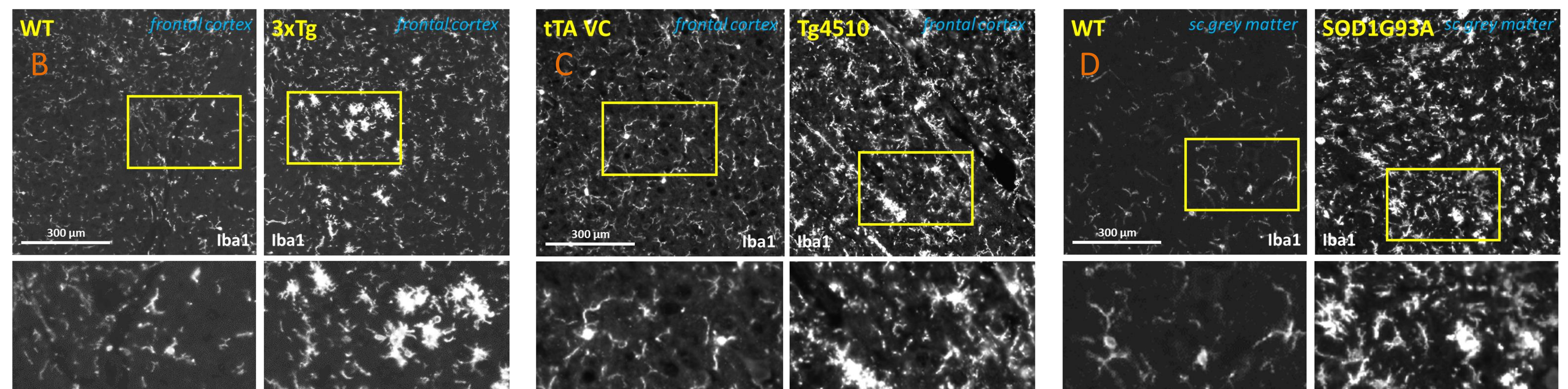## IMAGES OF MICROGLIAL MORPHOLOGICAL PATTERNS

**Figure 6:** (A) Microglia in Rett syndrome mice: Generally obvious is lower labeling in Mecp2+/- mice, whereas this is due to an overall lower expression of Iba1. The cutouts from the yellow rectangles show the WT in original visualization settings and the Mecp2 sample with enhancement. Notably the microglial morphology is not much changed and just the Iba1 signal leading to this impression. Measurements confirmed that the ramification in these mice is not different from WT controls, while signal was reduced as well as only very few activated cells can be found in the state of immunodeficiency.

**Figure 7:** (B) Comparison of typical microglia in 3xTg AD mice versus wild type (WT): Amyloid deposition leads to clustering of cells and cytosis, whereas cells in those clusters are frequently hypertrophic and at early stage. Singular cells unrelated to amyloid depositions are often de-ramifying. (C) Comparison of typical microglia in Tg4510 mice versus tTA controls: Neuron loss leads to atrophy and a strong increase of microglia density. Cells are often hypertrophic and also hyper-ramifying. (D) Comparison of typical microglia in SOD1G93A ALS mice versus WT: The dominant microglia is hypertrophic with clear signs of de-ramification thus short processes with little branching. In this model the cytosis is enormous.

## CONCLUSION

In summary, we demonstrate that we are able to distinguish the type of disease by patterns of microglial alterations in models to four disease types: AD, Tauopathy, Rett Syndrome and ALS. Those data suggest to further rethink the hitherto theory and argue for in deep analyses of the dominant and subdominant morphologies of microglia to find the links of these patterns to the basic pathological stimuli (APP, Tau, SOD1 mutation or Mecp2 insufficiency). Which mechanisms are responsible for the diversity of microglial reactivity patterns in different disease types? How many other neurodegenerative diseases produce different microglia patterns? Even more, pattern changes over age in the different models could give us valuable new insights to triggers of neuroinflammatory events coupled with morphological microglial alterations during disease progression. Additional in house data have already shown that patterns can change during ageing in the models. As well additional SBA and classifications turned out to be much more sensitive to treatment induced changes than the classical Iba1 evaluations alone in detecting compound effects. Last but not least to our mind an imperative task would be to compare these patterns with those found in human samples to explore the translational aspects from mouse models to the characteristics of human microglia in various brain disorders.